S. Afr. J. Chem., 2008, **61**, 157–161,
<http://journals.sabinet.co.za/sajchem/>.

Performance and Structure of $LiNi_{0.5}Mn_{1.5}O_4$ Prepared from Various Ni Precursors for Lithium Ion Batteries

Zhaoyong Chen[a], Shan Ji[b]*, Huali Zhu[a], Sivakumar Pasupathi[b], Ben Bladergroen[b] and Vladimir Linkov[b]

[a]*Department of Materials Science and Engineering, Changsha University of Science and Technology, Changsha, 410076, People's Republic of China*
[b]*South African Institute for Advanced Materials Chemistry, University of the Western Cape, Bellville, 7535 South Africa*

Received 21 August 2007, revised 6 May 2008, accepted 12 November 2008

ABSTRACT

$LiNi_{0.5}Mn_{1.5}O_4$ compounds were prepared through a solid-state reaction using various Ni precursors. The effect of the precursors on the electrochemical performance of $LiNi_{0.5}Mn_{1.5}O_4$ was investigated. $LiNi_{0.5}Mn_{1.5}O_4$ made from $Ni(NO_3)_2 \cdot 6H_2O$ shows the best charge-discharge performance. The reversible capacity of $LiNi_{0.5}Mn_{1.5}O_4$ is about 145 mA h g^{-1} and remained at 143 mA h g^{-1} after 10 cycles at 3.0 to 5.0 V. The XRD results showed that the precursors and dispersion method had significant effects on their structures. Pure spinel phase can be obtained with a high energy ball-milling method and $Ni(NO_3)_2 \cdot 6H_2O$ as precursor. A trace amount of the NiO phase was detected in $LiNi_{0.5}Mn_{1.5}O_4$ with the manual grinding method when $Ni(CH_3COO)_2 \cdot 6H_2O$, NiO and Ni_2O_3 were used as precursors.

KEYWORDS

$LiNi_{0.5}Mn_{1.5}O_4$, spinel, cathode materials, lithium ion battery.

1. Introduction

$LiNi_{0.5}Mn_{1.5}O_4$ is considered as one of the most promising cathode materials for substituting $LiCoO_2$ because of its high specific capacity, low cost, low toxicity, high stability, and highly reversible discharge capacity at 5 V.[1–5] Although spinel $LiMn_2O_4$ as cathode for Li ion batteries has the advantage of low cost and safety, the Mn^{3+} in this compound decreases the stability of charge/discharge cycles due to deformation of the crystal structure. Also, the stability of $LiMn_2O_4$ would further drop due to the dissolution of manganese in the electrolyte, especially at high temperature.[4–6]

In $LiNi_{0.5}Mn_{1.5}O_4$, Mn^{4+} forms the lattice frame of the crystal and Ni^{2+} is responsible for redox, which could stabilize this compound and facilitate intercalation/de-intercalation and diffusion of Li ions during cycling.[7–9] However, the solid-state reaction used commonly to prepare $LiNi_{0.5}Mn_{1.5}O_4$ is not adequate to control the composition of Ni and Mn, and produces an impurity in the form of NiO. The capacity of $LiNi_{0.5}Mn_{1.5}O_4$ prepared through solid-state reaction is only 120 mA h g^{-1}. In order to obtain a high purity spinel phase, various synthetic methods have been developed. Pure $LiNi_{0.5}Mn_{1.5}O_4$ spinel, with high electrochemical performance was prepared *via* a co-precipitation and sol-gel method by Liquan and co-workers,[10–12] but was limited to small-scale production. The effects of substituting manganese ions with other metal ions and the partial pressure of oxygen on the structural stability of the spinel were documented recently.[13,14] The irreversible capacity loss that impairs cyclability, however, resulted from substitution of the manganese ion, which leads to the formation of the unexpected valences of Ni and Mn, such as Ni^{3+} and Mn^{3+}. A systematic study on the effect of precursors and mixing method on structure and performance of cathodes prepared *via* solid-state reaction has not yet been reported. The goal of this work was to study the effect of high energy ball-milling and various Ni precursors on the structure and electrochemical performance of $LiNi_{0.5}Mn_{1.5}O_4$ in order to obtain high purity $LiNi_{0.5}Mn_{1.5}O_4$ spinel by means of a solid state reaction method.

* To whom correspondence should be addressed. E-mail: sji@uwc.ac.za

2. Experimental

2.1. Materials

Separator Celgard 2400 was purchased from Celgard, Inc., Charlotte, NC, USA. All the other materials supplied by Aldrich, St Louis, MO, USA, were used without further purification.

2.2. Preparation of $LiNi_{0.5}Mn_{1.5}O_4$

The stoichiometric amounts of the precursors were weighed accurately, i.e. 37.10 g of $Ni(NO_3)_2 \cdot 6H_2O_3$, 34.67 g of MnO_2 and 9.43 g of Li_2CO_3, and mixed with anhydrous ethanol as the dispersion medium. The mixture was allowed to ball-mill in a planetary micro-mill or was manually ground for 6 h at room temperature. The milled mixture was dried and calcined at 750 °C for 20 h. $Ni(CH_3COO)_2 \cdot 6H_2O$, NiO and Ni_2O_3 were also used as Ni precursors to prepare $LiNi_{0.5}Mn_{1.5}O_4$. The samples made from different Ni precursors are listed in Table 1.

2.3. Characterization

X-ray phase analysis was carried out on a Rigaku/Max-RA X-ray powder diffractometer (Salem, NC, USA) with CuK_α radiation. The scan range was $10 < 2\theta < 70$ °, and a step of 0.02 ° was used. The voltage and current were 30 kV and 100 mA, respectively.

2.4. Charge/Discharge Test

The resulting $LiNi_{0.5}Mn_{1.5}O_4$ was mixed with acetylene black, polyvinylidene difluoride (PVDF) (mass ratio of $LiNi_{0.5}Mn_{1.5}O_4$,

Table 1 Samples prepared from different Ni precursors and mixing methods.

Sample label	Ni source	Mixing methods
A	$Ni(NO_3)_2 \cdot 6H_2O$	Ball-milling
A1	$Ni(NO_3)_2 \cdot 6H_2O$	Manual grinding
B	$Ni(CH_3COO)_2 \cdot 6H_2O$	Ball-milling
C	NiO	Ball-milling
D	Ni_2O_3	Ball-milling

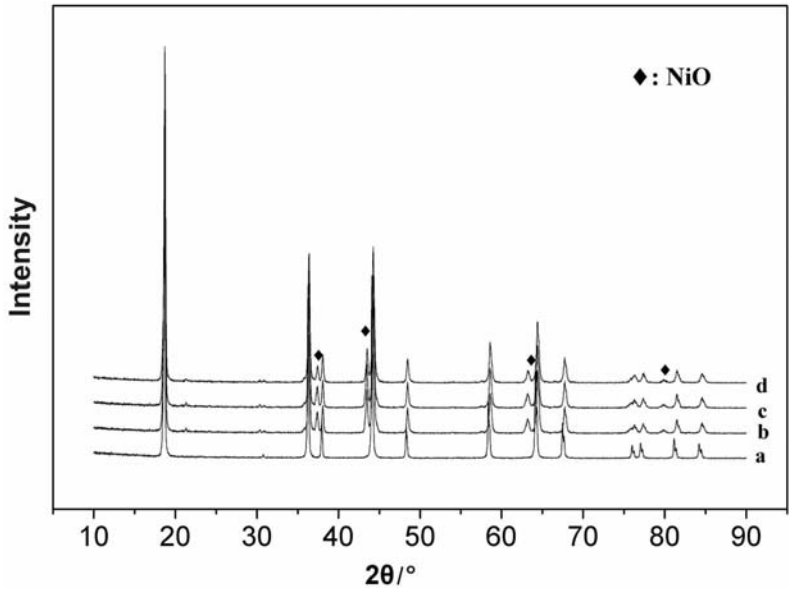

Figure 1 XRD patterns of $LiNi_{0.5}Mn_{1.5}O_4$: (a) sample A; (b) sample B; (c) sample C; (d) sample D.

acetylene black and PVDF was 80:10:10) in 1-methyl-2-pyrrolidinone (NMP) onto an Al foil (as current collector). The electrodes were dried and pressed with a hydraulic press. Li ion secondary cells were assembled by using lithium sheet as the anode and the above prepared electrodes as cathodes. Celgard 2400 was used as separator which was soaked in electrolyte, i.e. 1 mol L^{-1} $LiPF_6$ solution in an ethylene carbonate (EC) and dimethyl carbonate (DMC) mixed solvent (1:1 v/v ratio). The cells were assembled in an argon-protected glove box. The charge/discharge studies were carried out by using a Land-BTL10 (Wuhan, China) automatic battery test system.

3. Results and Discussion

3.1. XRD Analysis of $LiNi_{0.5}Mn_{1.5}O_4$

During calcinations of milled mixtures, the partial pressure of oxygen must be controlled very carefully; otherwise, Li_2MnO_3 or $LiMnO_2$ would be formed in the sample. This prevents a part of the Ni from entering the lattice of $LiNi_{0.5}Mn_{1.5}O_4$ spinel and thereby forms NiO. In our preparations, all the samples were calcined in air. $LiNi_{0.5}Mn_{1.5}O_4$ spinel with only traces of NiO was obtained without any control of partial pressure of oxygen but by using electrolytic MnO_2 instead of chemical MnO_2. The XRD patterns of $LiNi_{0.5}Mn_{1.5}O_4$ made from $Ni(NO_3)_2 \cdot 6H_2O$, $Ni(CH_3COO)_2 \cdot 6H_2O$, NiO and Ni_2O_3, which were ball-milled and calcined at the same temperature, are compared in Fig. 1. Among them, only the $LiNi_{0.5}Mn_{1.5}O_4$ made from $Ni(NO_3)_2 \cdot 6H_2O$ shows the pure spinel structure compared with the standard pattern (JCPDS: 35-0782). Weak impurity peaks of NiO at 2θ = 37.5 °, 68.2 ° and 80.0 ° were detected in the XRD patterns of all the other $LiNi_{0.5}Mn_{1.5}O_4$ samples. Although there is a trace of NiO, their XRD patterns show the standard spinel structure. The amounts of NiO are lower than those reported by Kim[8] using a solid-state reaction and very close to the sample prepared *via* a co-precipitation method. We presume that there are two reasons why high purity $LiNi_{0.5}Mn_{1.5}O_4$ can be prepared by ball-milling from $Ni(NO_3)_2 \cdot 6H_2O$ as a Ni precursor. Firstly, the ball-milling could decrease activation energy, which would facilitate the formation of spinel; secondly, the oxygen formed by decomposition of $Ni(NO_3)_2 \cdot 6H_2O$ would restrain impurities formed in $LiNi_{0.5}Mn_{1.5}O_4$.

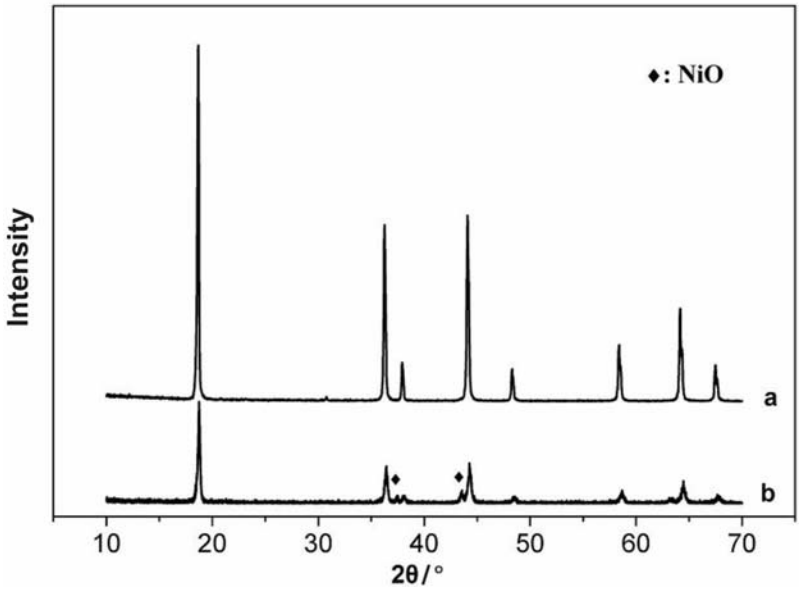

Figure 2 XRD patterns of $LiNi_{0.5}Mn_{1.5}O_4$: (a) sample A; (b) sample A1.

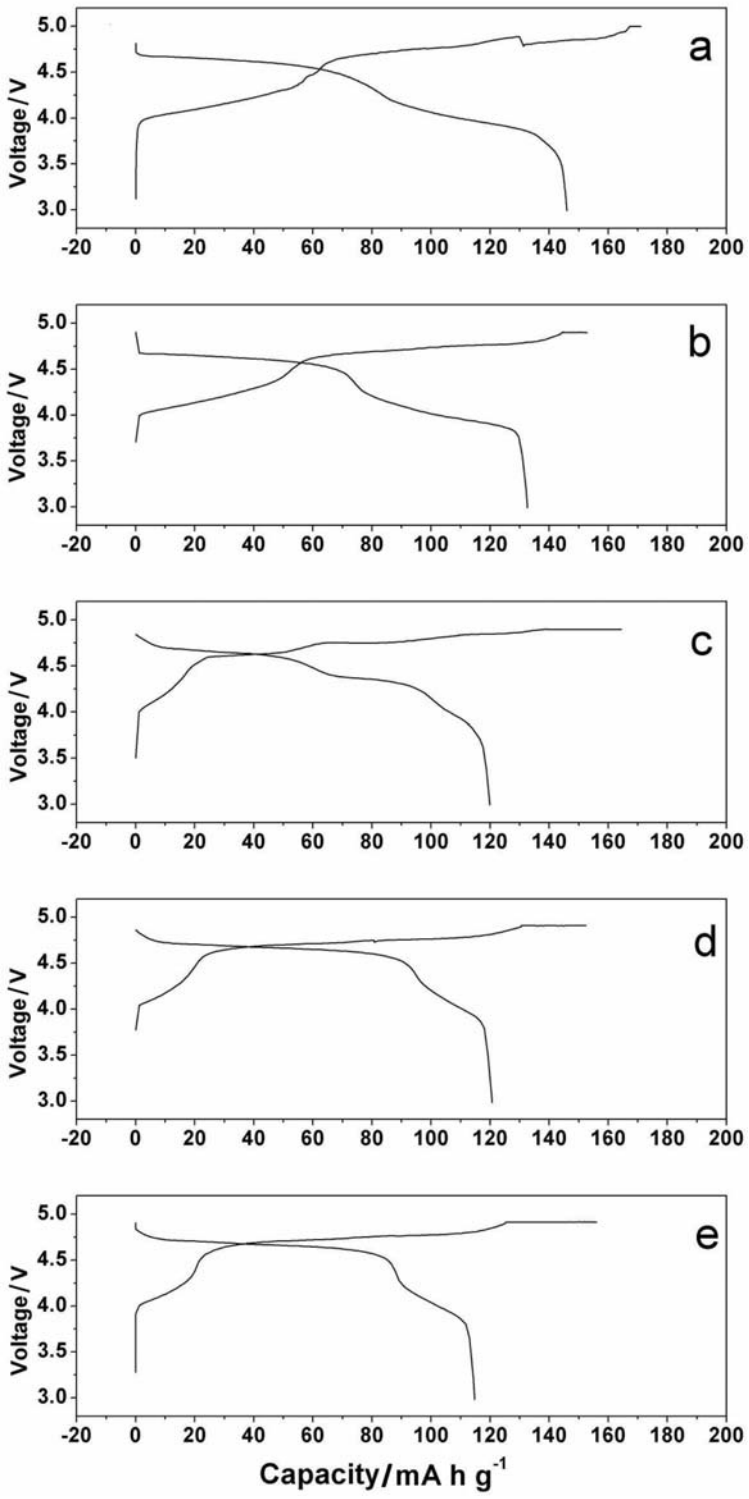

Figure 3 Voltage *versus* initial capacity: (**a**) sample A, 3.0–5.0 V; (**b**) sample A, 3.0–4.9 V; (**c**) sample B, 3.0–4.9 V; (**d**) sample C, 3.0–4.9 V; (**e**) sample D, 3.0–4.9 V.

The XRD patterns of $LiNi_{0.5}Mn_{1.5}O_4$, prepared by ball-milling and manual grinding, are shown in Fig. 2. $LiNi_{0.5}Mn_{1.5}O_4$ prepared by ball-milling shows the pure spinel structure without any impurity peaks in the XRD pattern. However, obvious impurity peaks of NiO are noted in the $LiNi_{0.5}Mn_{1.5}O_4$ ground manually. Moreover, the intensities of the peaks of sample A are much stronger than those of sample A1, which indicates that ball-milling could facilitate the crystallization of $LiNi_{0.5}Mn_{1.5}O_4$. It is concluded that milling methods have a significant effect on the structure of $LiNi_{0.5}Mn_{1.5}O_4$.

3.2. Electrochemical Performances of $LiNi_{0.5}Mn_{1.5}O_4$

The $LiNi_{0.5}Mn_{1.5}O_4$ cathode has two charge/discharge voltage plateaus, i.e. at 4 V and 5 V. The plateau at 4 V was caused by the Mn^{3+}/Mn^{4+} redox couple and that at 5 V by Ni^{2+}/Ni^{4+}. When there are more Mn^{4+} ions than Ni^{2+} in $LiNi_{0.5}Mn_{1.5}O_4$, then the corresponding capacity at 4 V will be smaller and that at 5 V will be larger, and *vice versa.* Figures 3a and 3b show the charge-discharge voltage profiles of $LiNi_{0.5}Mn_{1.5}O_4$ in the voltage ranges of 3.0 to 5.0 V and 3.0 to 4.9 V, respectively. In Fig. 3a, there is a rapid voltage drop at 4.9 V and then the voltage increases slowly

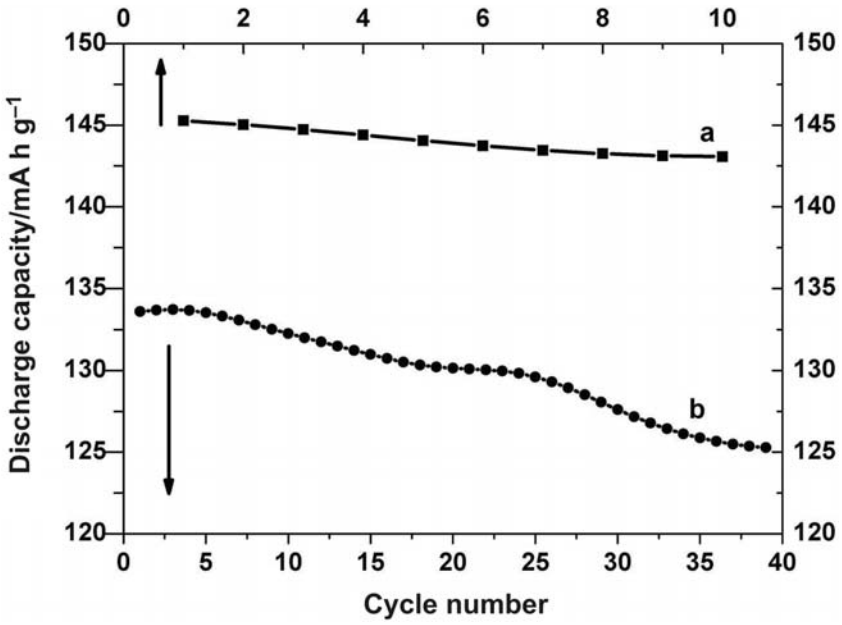

Figure 4 Capacity *versus* cycle number of sample A: (a) 3.0–5.0 V; (b) 3.0–4.9 V.

during the course of charge. This could be caused by oxidation of the electrolyte, which will result in an abrupt increase of current similar to the shortcut of a battery. With this electrolyte, it is better to charge/discharge in the voltage range of 3.0 to 4.9 V. During the charge, two voltage plateaus were observed at 4.3 and 4.8 V. The ratio of the corresponding capacities of 4.3 and 4.8 V is 1:2 during charging and 1:1 during discharge.

Compared with sample A, the initial capacity of $LiNi_{0.5}Mn_{1.5}O_4$ made from $Ni(CH_3COO)_2 \cdot 6H_2O$ (sample B) dropped to 120 mA h g^{-1} (Fig. 3c). There are three voltage plateaus (at 4.0, 4.4 and 4.6 V) in the voltage profile of sample B, but only two plateaus in that of sample A. The ratio of the corresponding capacities at 4.0, 4.4 and 4.6 V is 1:2:3. The voltage profiles of $LiNi_{0.5}Mn_{1.5}O_4$ made from NiO and Ni_2O_3 are similar. The plateau at 4 V is much smaller and almost disappears in comparison with that of sample A. The capacities at the 4.6 V and 4 V plateaus are 95 and 15 mA h g^{-1}, respectively. It is obvious that the amounts of Mn^{3+} and Ni^{3+} decrease, and Mn and Ni tend to form Mn^{4+} and Ni^{2+} in $LiNi_{0.5}Mn_{1.5}O_4$, when metal oxides were used as Ni precursors.

Figure 4 shows the variation in the discharge capacity of samples A and B, as a function of the number of cycles at different voltage ranges. The reversible discharge capacity of sample A at 3.0 to 5.0 V is 11 mA h g^{-1} higher than that at 3.0 to 4.9 V. The discharge capacity is up to 145 mA h g^{-1} when the cut-off voltage is 5.0 V. The discharge capacity is up to 133 mA h g^{-1} when the cut-off voltage is 4.9 V. At 3.0 to 5.0 V, sample A shows high stability with the discharge capacity dropping marginally to 142 mA h g^{-1} after 10 cycles. However, at 3.0 to 4.9 V, the discharge capacity drops to 124 mA h g^{-1} after 40 cycles. Also, for sample A, similar discharge capacity fading was observed at different voltage ranges.

$LiNi_{0.5}Mn_{1.5}O_4$, made from various Ni precursors also shows excellent stability. The capacity retention rates of samples A, B, C and D were 97.40 %, 90.50 %, 89.71 % and 97.43 %, respectively (Fig. 5). This showed that $LiNi_{0.5}Mn_{1.5}O_4$ made from $Ni(NO_3)_2 \cdot 6H_2O$ and Ni_2O_3 has a good capacity retention rate. The capacity retention rate of $LiNi_{0.5}Mn_{1.5}O_4$ made from NiO is the lowest.

The effect of milling methods on cycle life and coulomb efficiency of $LiNi_{0.5}Mn_{1.5}O_4$ made from $Ni(NO_3)_2 \cdot 6H_2O$ is shown in

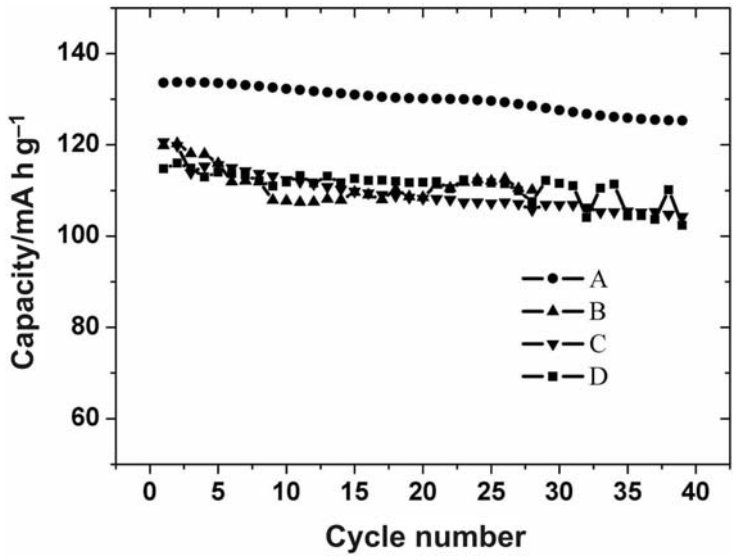

Figure 5 Capacity *versus* cycle number of samples A, B, C and D (3.0–4.9 V).

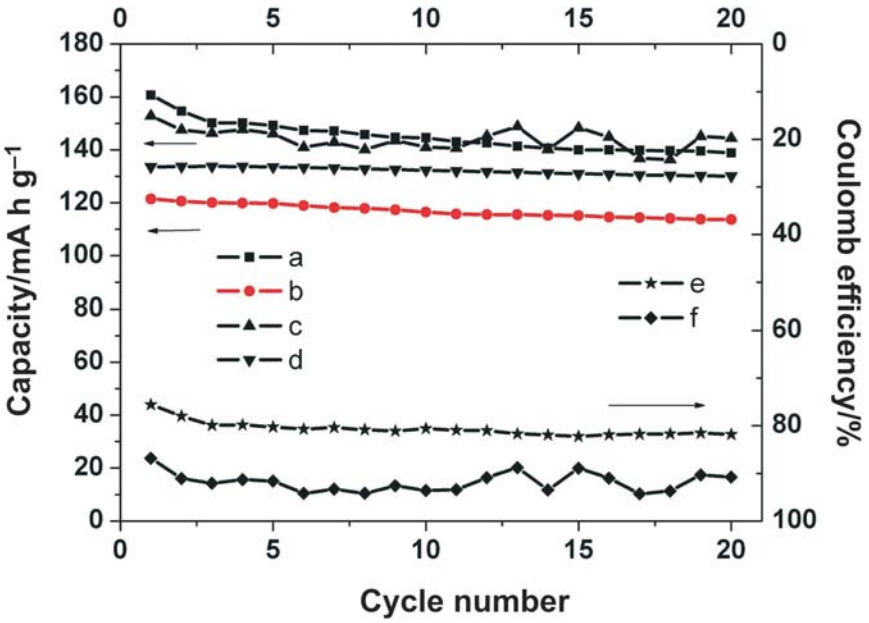

Figure 6 Capacity and Coulomb efficiency *versus* cycle number of samples A and A1 (a, b and c, d are the charge-discharge cycle curves of samples A1 and A, respectively; e, f are the Coulomb efficiency curves of A1 and A, respectively).

Fig. 6. The initial capacity of the ball-milled sample is 12 mA h g^{-1} higher than that of manually ground sample. The coulomb efficiency of the ball-milled sample is 10 % higher than that of the manually ground sample. The charge capacities of both samples are very close, but there is an obvious difference between discharge capacities. This suggests that the Li ion intercalation/de-intercalation is faster in the ball-milled sample. The capacity retention rate and stability of the ball-milled sample are better than those of the manually ground sample in the first 20 cycles.

4. Conclusion

$LiNi_{0.5}Mn_{1.5}O_4$ spinel, a promising cathode material with high reversible capacity and stability, has been prepared by solid-state reaction. The crystal structure was characterized by XRD. Among the $LiNi_{0.5}Mn_{1.5}O_4$ cathode materials made from various Ni precursors, $LiNi_{0.5}Mn_{1.5}O_4$ made from $Ni(NO_3)_2 \cdot 6H_2O$ has the best electrochemical performance. With $Ni(NO_3)_2 \cdot 6H_2O$ as the Ni precursor and ball-milling, high purity spinel $LiNi_{0.5}Mn_{1.5}O_4$ can be prepared *via* a solid-state reaction. Therefore, it has the potential to substitute currently applied complicated preparation methods like co-precipitation, sol-gel and spray pyrolysis methods for producing high purity $LiNi_{0.5}Mn_{1.5}O_4$. The $LiNi_{0.5}Mn_{1.5}O_4$ electrode shows a high initial discharge capacity of 145 mA h g^{-1} and a very stable cycling performance. The discharge capacity still remained at 142 mA h g^{-1} after 10 cycles.

Acknowledgements

Financial assistance from the Department of Science and Technology, South Africa, is gratefully acknowledged.

References

1 R. Alcantara, M. Jaraba, P. Lavela, J.M. Lloris, P. Vicente and J.L. Tirado, *J. Electrochem. Soc.,* 2004, **151**, 53–58.
2 A. Caballero, L. Hernan, M. Melero, J. Morales and M. Angulo, *J. Electrochem. Soc.,* 2005, **152**, 6–12.
3 H. Sang and K. Yang, *Electrochim. Acta,* 2004, **50**, 431–434.
4 Y. Xia, H. Zhou and M. Yoshio, *J. Electrochem. Soc.,* 1997, **144**, 2593–2600.
5 H. Dong and M. Seung, *J. Electrochem. Soc.,* 1997, **144,** 3342–3347.
6 A. Pasquier, A. Blyr, P. Courjal, D. Larcher, G. Amatucci, B. Gérand and J.M. Tarascon, *J. Electrochem. Soc.,* 1999, **146**, 428–436.
7 A. Eftekhari, *J. Power Sources,* 2003, **124**, 182–190.
8 J. Kim, S. Myung and Y. Sun, *Electrochim. Acta,* 2004, **49**, 219–227.
9 B. Markovsky, Y. Talyossef, G. Salitra, D. Aurbach, H. Kim and S. Choi, *Electrochem. Comm.,* 2004, **6**, 821–826.
10 Y. Sun, Z. Wang, X. Huang and L. Chen, *J. Power Sources,* 2004, **132,** 161–165.
11 S. Mukerjee, X.Q. Yang, X. Sun, S.J. Lee, J. McBreen and Y. Ein–Eli, *Electrochim. Acta,* 2004, **49**, 3373–3382.
12 Y. Idemoto, H. Narai and N. Koura, *J. Power Sources,* 2003, **119,** 125–129.
13 R. Alcantara, M. Jaraba, P. Lavela, J.M. Lloris, V.C. Pérez and J.L. Tirado, *J. Electrochem. Soc.,* 2005, **152**, 13–18.
14 V.C. Pérez, J. Lloris and J. Tirado, *Electrochim. Acta,* 2004, **49**, 1963–1967.